

SLAC-PUB-3095

April 1983

(T/E)

**COMPOSITE MODELS AND FINITE WIDTH EFFECTS
ON $e^+e^- \rightarrow \mu^+\mu^-$ ASYMMETRY***

PISIN CHEN

*Department of Physics, University of California
Los Angeles, California 90024*

Z. REK[†] AND F. M. RENARD

*Stanford Linear Accelerator Center
Stanford University, Stanford, California 94305*

ABSTRACT

We investigate the possibility of distinguishing standard model from composite models at an intermediate energy range ($45 \sim 60$ GeV). We show that effects due to multiple neutral weak bosons and their finite widths can be observable in $e^+e^- \rightarrow \mu^+\mu^-$ forward-backward asymmetry.

Submitted to Physical Review D

*Work supported in part by the Department of Energy, contract DE-AC03-76SF00515 and by Centre National de la Recherche Scientifique, France.

[†]On leave of absence from Warsaw University Branch, Bialystok, Poland.

1. Introduction

The discovery of W^\pm and Z^0 bosons at CERN¹ is a monumental progress in the study of electroweak interactions. However the whole picture of electroweak interactions is not yet settled. In particular the structure of the weak neutral current is still far from precise. Namely¹

$$M_W = 80.9 \pm 1.5 \text{ GeV}, \quad M_Z = 95.1 \pm 1.4 \text{ GeV}; \quad \Gamma \leq 7 \text{ GeV} \text{ from UA1}$$

$$M_W = 81.0 \pm 2.5 \text{ GeV}, \quad M_Z = 91.2 \pm 0.9 \text{ GeV}; \quad \Gamma \leq 7 \text{ GeV} \text{ from UA2} .$$

These results are consistent with the standard model predictions but the low statistics in the events still leaves room for small departure in the Z^0 mass and for substantially larger width. Furthermore even if the mass and the width are close to the standard values this does not mean that Z^0 is necessarily a gauge particle. Further tests are necessary in order to precise the nature of these weak bosons. The most accurate information on Z^0 width and couplings should come from direct production in e^+e^- collisions. Unfortunately several more years are needed before we can reach the necessary energy. In this paper we demonstrate that $e^+e^- \rightarrow \mu^+\mu^-$ asymmetry at lower energy (e.g. 45 GeV from PETRA and 60 GeV from TRISTAN) can provide useful clues towards the nature of the Z^0 boson.

There are proposals of composite leptons, quarks and weak bosons² as alternatives to the standard model. These composite models offer different predictions on the neutral current amplitudes. In particular, for those composite models with low mass scales (say $\Lambda \leq 1 \text{ TeV}$), the low energy neutral current phenomenology may differ from the standard predictions. The differences come from the existence of more neutral bosons which appear either as excited states of the Z boson or as isoscalar partners of the low lying isovector weak bosons. In addition, there will be width effects from each neutral weak boson. Abbott and Farhi³ and Fritzsche and Mandelbaum⁴ argue that the widths of composite weak bosons might behave similarly to the ordinary resonances

and hence be quite sizeable. On the other hand, even if the widths are as narrow as the standard predictions (~ 3 GeV), there are still some subtle effects expected from the compositeness. There should be new phenomena above some threshold (of the order of Λ), such as productions of exotic leptons and quarks, the jets associated with the preons, etc. These new channels will modify the weak boson propagators through their contribution to the vacuum polarization.

In this paper we show that it is possible to distinguish the standard model from the composite models through the $e^+e^- \rightarrow \mu^+\mu^-$ process at the intermediate energy range (45 GeV \sim 60 GeV). The advantages of our approach are twofold: experimentally $e^+e^- \rightarrow \mu^+\mu^-$ provides a clean information, and theoretically this process is easy to describe directly in terms of weak boson propagators.

We will concentrate on the $e^+e^- \rightarrow \mu^+\mu^-$ cross section σ and forward-backward asymmetry A_{FB} . So far calculations have been done by Hollik and others⁵ only in the framework of standard and extended gauge models. To extract the possible composite effects we need a more general treatment.

The contents of our paper are the following: In Sec. 2 we derive a generalized formula for the amplitude of a general neutral current process $e^+e^- \rightarrow f\bar{f}$ passing through a photon and a series of weak bosons. This formula involves the modified weak boson propagators due to finite width effects. In Sec. 3 we study the structure of $e^+e^- \rightarrow \mu^+\mu^-$ amplitude. Sum rules for coupling and mass parameters are given by comparison with low energy phenomenology. Two types of illustrations are then discussed where one describes a single Z boson case and the other deals with Z and an additional boson Y . The results are given in Sec. 4. The calculations are carried out at $\sqrt{s} = 45$ GeV and $\sqrt{s} = 60$ GeV. A discussion of how future experiments can help to distinguish different electroweak models is given at the end.

2. Finite Width Effects

Since we are concerned with the effects due to the broad weak-bosons widths, the normal Breit-Wigner shape of resonance propagator should be modified. There are obvious effects coming from the phase space, and there are also constraints from analyticity and unitarity that the weak-boson amplitudes should satisfy. These are well-known features for resonances in hadronic physics.⁶ This kind of modification also appears when one considers higher order corrections in QED and QFD,⁷ though the magnitude of the corrections is generally small (of the order of $\frac{\alpha}{\pi}$).

Finite width effects will in general modify the electroweak mixing scheme by appearance of complex and energy-dependent couplings and mixing angles. In the present work, as we are mainly interested in the energy range reachable by PETRA and TRISTAN which is below the possible resonance peak of the weak-boson, we shall keep only the leading effects. We consider each weak-boson propagator independently and neglect the phases (small at the low-energy) which come from finite width treatment of the non-diagonal mixing terms. We do not consider the modifications of the photon propagator; we assume that the main effects (of the type of vacuum polarization) are included in the radiative correction programs used when analyzing the experimental events.

After mixing with γ and other bosonic states each physical boson acquires an inverse propagator

$$D_0(s) = m^2 - s + \Sigma(s) \tag{2.1}$$

where m would be its physical mass when neglecting the couplings to decay channels. $\Sigma(s)$ is precisely the additional contribution due to the processes of Fig. 1. The physical mass M is now given by the condition

$$\text{Re}D_0(M^2) \equiv m^2 - M^2 + \text{Re}\Sigma(M^2) = 0 \quad . \quad (2.2)$$

The inverse propagator can then be written

$$D_0(s) = [1 - \Sigma'(M^2)] D(s) \quad (2.3)$$

where

$$D(s) \equiv M^2 - s + \Pi(s) - iM\Gamma(s) \quad (2.4)$$

having defined

$$\Sigma'(M^2) \equiv \left\{ \frac{d}{ds} \text{Re}\Sigma(s) \right\}_{s=M^2} \quad (2.5)$$

$$\Pi(s) \equiv \frac{\text{Re}\Sigma(s) - \text{Re}\Sigma(M^2) - (s - M^2)\Sigma'(M^2)}{1 - \Sigma'(M^2)} \quad (2.6)$$

$$M\Gamma(s) \equiv \frac{-\text{Im}\Sigma(s)}{1 - \Sigma'(M^2)} \quad (2.7)$$

For $s \simeq M^2$, $D(s)$ given by Eq. (2.4) agrees with the usual Breit-Wigner formula, because $\Pi(s)$ behaves like $(s - M^2)^2$ as can be seen from Eq. (2.6). The total width at the top of the resonance is $M\Gamma(M^2)$ given by Eq. (2.7). The factor $[1 - \Sigma'(M^2)]$ is a renormalization effect due to the decay channels (F).

Any amplitude describing this boson formation will be written as

$$R_{f_i}(s) = \frac{g_0^2}{D_0(s)} \equiv \frac{g^2}{D(s)} \quad , \quad (2.8)$$

where

$$g^2 \equiv g_0^2 [1 - \Sigma'(M^2)]^{-1} \quad (2.9)$$

and g_0 is the bare coupling constant. Electroweak amplitudes should be normalized at $s = 0$ according to the usual phenomenology which fixes $R_{f_i}(0)$ values (see more details from the sum rules in Sec. 3). However we have

$$R_{fi}(0) = \frac{g^2}{M^2 + \Pi(0)} \equiv \frac{g^2}{M^2(1 + \delta)} \quad (2.10)$$

which introduces the “finite width coefficient” δ

$$\delta = \frac{\Pi(0)}{M^2} = \frac{\text{Re}\Sigma(0) - \text{Re}\Sigma(M^2) + M^2\Sigma'(M^2)}{M^2[1 - \Sigma'(M^2)]} \quad (2.11)$$

Then

$$R_{fi}(s) = R_{fi}(0) \cdot \frac{M^2(1 + \delta)}{D(s)} \quad (2.12)$$

In the zero-width treatment one would have

$$R_{fi}(s) = \frac{g_0^2}{M^2 - s} = R_{fi}(0) \frac{M^2}{M^2 - s} \quad (2.13)$$

Comparing Eq. (2.12) and Eq. (2.13) we conclude that the leading finite width influence on a single boson propagator will be obtained by the following replacement

$$\frac{1}{M^2 - s} \Rightarrow \frac{1 + \delta}{M^2 - s + \Pi(s) - iM\Gamma(s)} \quad (2.14)$$

with δ , $\Pi(s)$ and $M\Gamma(s)$ given in Eq. (2.11), (2.6) and (2.7) in terms of the function $\Sigma(s)$. This replacement will not affect the various sum rules⁸ coming from zero energy normalizations given by charged current and neutral current phenomenology (see Sec. 3).

The amplitude of the neutral current process $e^+e^- \rightarrow f\bar{f}$ due to an exchange of a photon and a series ($i = 1, \dots, n$) of weak bosons will now take the general form:

$$\frac{e^2 Q_f}{s} \bar{v}_e \gamma^\mu u_e \bar{u}_f \gamma_\mu v_f + \sum_{i=1}^n \frac{1 + \delta_i}{D_i(s)} \bar{v}_e \gamma^\mu (a_{ei} - b_{ei}\gamma^5) u_e \bar{u}_f \gamma_\mu (a_{fi} - b_{fi}\gamma^5) v_f \quad (2.15)$$

where Q_f , a_{ei} , b_{ei} , a_{fi} , b_{fi} are the charge, the vector couplings and the axial couplings of the fermions (see Appendix for the general formulae on cross sections and asymmetries).

The effects of the replacement (2.14) are threefold. Firstly, there is the $(1 + \delta)$ factor in the numerator which changes the magnitude of the amplitudes for $s \neq 0$. For example, at $s = M^2$ this factor gives precisely the difference between the usual Breit-Wigner formula $M^2 - s - iM\Gamma$ and the actual formula. Secondly, the real part of the propagator is modified by the additional term $\Pi(s)$. Thirdly, the imaginary part of the propagator (the width term $M\Gamma(s)$) has an energy dependence controlled by the phase space of the opened channels (F).

In order to quantitatively estimate these effects we use the analytic properties of $\Sigma(s)$ and write the dispersion integral following from definitions (2.6) and (2.7)

$$\Pi(s) = -\frac{(s - M^2)^2}{\pi} \text{Re} \int_{s_0}^{\infty} \frac{M\Gamma(s')}{(s' - s)(s' - M^2)^2} ds' \quad (2.16)$$

with $M\Gamma(s') \equiv \Sigma_{(F)} M\Gamma_F(s')$. s_0 is the threshold of the lowest lying channel (F) coupled to the weak boson. We have then from (2.11)

$$\delta \equiv \frac{\Pi(0)}{M^2} = -\frac{M^2}{\pi} \int_{s_0}^{\infty} \frac{M\Gamma(s')}{s'(s' - M^2)^2} ds' . \quad (2.17)$$

To illustrate this point let us look at two extreme cases. If the dominant channels are fermion pairs with negligible mass we can see from Eq. (2.16) and (2.17) that $\Pi(s)$ (for $s < M^2$) and δ get positive values. On the other hand if the dominant channels have high thresholds ($s_0 \geq M^2$) these quantities will get negative values.

In the first case we can approximate the energy dependence of the width by

$$M\Gamma(s) \simeq \left(\frac{s}{M^2}\right) M\Gamma(M^2) . \quad (2.18)$$

Then from Eq. (2.16)

$$\Pi(s) \simeq \delta \left[M^2 - s \left(1 + \log \frac{M^2}{s} \right) \right] \quad (2.19)$$

with

$$\delta \equiv \frac{\Pi(0)}{M^2} = \frac{\Gamma(M^2)}{\pi M} . \quad (2.20)$$

All the finite width effects in Eq. (2.14) can then be expressed in terms of $\delta = \Gamma(M^2)/\pi M$. To appreciate their importance we can first take the standard case with $M \simeq 90$ GeV and $\Gamma(M^2) \simeq 3$ GeV. This gives $\delta \simeq 0.01$. If the width is much larger due to the presence of, e.g., a large number of generations, supersymmetric partners, or composite model effects, then δ could be much larger. For example $\Gamma(M^2) \simeq 10$ GeV gives $\delta \simeq 0.03$.

The second case could happen if the weak boson is composite with a scale $\Lambda > M$. One expects many new effects to appear for $s \geq \Lambda^2$, in particular the opening of multifermion, multiphoton, multigluon channels ...etc. From (2.16) and (2.17) one observes that they will give contributions to $\Pi(s)$ and δ of the order of $-(M^2/\pi\Lambda^2)$. The lowest mass scale among the present composite models is of the order of 250 GeV.² This means that one cannot expect δ to be less than -0.1 .

Without a precise model giving the threshold values s_F and the contributions $M\Gamma_F(s')$ it is impossible to give a definite prediction for δ . Nevertheless from the above discussion it appears that a reasonable range for δ is

$$-0.1 \leq \delta \leq +0.1 .$$

In the following we shall limit ourselves to three different illustrations, namely $\delta = \Gamma(M^2)/\pi M$, $\delta = 0$ and $\delta = -0.1$.

3. The Structure of $e^+e^- \rightarrow \mu^+\mu^-$ Amplitude

In this section we shall study the scattering amplitude of $e^+e^- \rightarrow \mu^+\mu^-$. The general amplitude involving a photon and several weak-bosons was given in Eq. (2.15).

For the sake of illustration we shall limit ourselves to two neutral weak-boson states, with the lighter one being the usual Z -boson. We shall call the heavier one the Y -boson though it could either be an isovector (e.g., the excited state of Z) or an isoscalar (e.g., the partner of Z in some composite models).

In Eq. (2.15) the couplings of $Z\ell^+\ell^-$ and $Y\ell^+\ell^-$ are not specified, and it can cover any extended gauge model⁸ or composite model mixing scheme.^{9,10} By imposing universality of couplings to fermion generations (i.e., the same couplings for e^+e^- and $\mu^+\mu^-$), we are left with eight parameters in the amplitude, namely, the masses M_Z , M_Y and widths Γ_Z , Γ_Y of the two weak-bosons, plus the vector and axial-vector coupling coefficients a_1 , a_2 and b_1 , b_2 , respectively.

However, these eight parameters are subject to the constraints from low energy phenomenology of weak neutral currents. At $s = 0$, we must identify Eq. (2.15) with

$$\frac{8G}{\sqrt{2}}\rho \left[(j_3 - \sin^2\theta_W j_{em})^2 + C j_{em}^2 \right] \quad (3.1)$$

where the weak isovector current is

$$j_3 = \gamma^\mu \left(\frac{1 - \gamma^5}{2} \right) I_3 \quad ,$$

and the electromagnetic current is

$$j_{em} = \gamma^\mu Q_f \quad .$$

By comparing term by term Eq. (2.15) and Eq. (3.1) we get the following constraints:

1. From the axial-vector – axial-vector term,

$$\frac{G\rho}{2\sqrt{2}} = \frac{b_1^2}{M_Z^2} + \frac{b_2^2}{M_Y^2} \quad , \quad (3.2)$$

2. From the vector-axial-vector term,

$$\frac{2G\rho}{\sqrt{2}} \sin^2\theta_W = \frac{b_1(b_1 - a_1)}{M_Z^2} + \frac{b_2(b_2 - a_2)}{M_Y^2} \quad , \quad (3.3)$$

3. And, from the vector-vector term,

$$C \left(\frac{8G\rho}{\sqrt{2}} \right)^2 = \frac{16(a_1 b_2 - a_2 b_1)^2}{M_Z^2 M_Y^2} . \quad (3.4)$$

Experimentally, we have $Gm_P^2 = 1.029 \times 10^{-5}$, $\rho = 1$, $\sin^2 \theta_W = 0.23$, and $C < 0.03$. This means we just have two strong constraints from Eq. (3.2) and Eq. (3.3). The last one (Eq. (3.4)) is actually an inequality.

The remaining freedom in the parameters is quite unrestricted. However it is reasonable^{1,8} to impose the condition that the average boson mass \bar{M} , defined by

$$\frac{1}{\bar{M}^2} \equiv \sum_{\ell=1}^2 \frac{b_\ell^2}{M_\ell^4} / \sum_{\ell=1}^2 \frac{b_\ell^2}{M_\ell^2} , \quad (3.5)$$

should lie within the range 92-100 GeV.

It will be clear in the later illustrations that the asymmetry effects are much more sensitive to the total width Γ_Z of the lighter boson than that of the heavier one. Hence, for the sake of simplicity we adopt a simple proportionality relation

$$\Gamma_Y = \frac{M_Y}{M_Z} \Gamma_Z . \quad (3.6)$$

At this point we are left with one free mass parameter from Eq. (3.5) and one width parameter from Eq. (3.6). As for the coupling coefficients, Eq. (3.2) to Eq. (3.4) still leave the relative strengths between Y and Z couplings unconstrained. We shall thus study the effects due to Y boson by looking at the extreme cases — either the Y boson is decoupled from the leptons or it has the same coupling strength as the Z boson.

In the decoupled extreme it is equivalent to having no Y boson, as we have our case 1,

1. Decoupled Y :

$$\bar{M} \equiv M_Z , \quad b_1 = \left[\frac{M_Z^2 G \rho}{2\sqrt{2}} \right]^{\frac{1}{2}} , \quad a_1 = b_1 (1 - 4 \sin^2 \theta_W) . \quad (3.7)$$

Obviously $C = 0$ in this case, and we are left with two free parameters M_Z and Γ_Z . Note that this case can accommodate the standard model.

In the second extreme there could be several possibilities. Even if Y and Z bosons have the same basic coupling strength they still can mix with the γ differently. With this in mind we consider the following four cases:

2. Same $\gamma - Y$ and $\gamma - Z$ mixings:

$$a_1 = a_2 = b_1(1 - 4 \sin^2 \theta_W) ,$$

and

$$b_1 = b_2 = \left[\frac{G\rho}{2\sqrt{2}} \cdot \frac{M_Z^2 M_Y^2}{M_Z^2 + M_Y^2} \right]^{\frac{1}{2}} ,$$

$$M_Y^2 = \frac{M_Z^4 + \left[M_Z^8 + 4M_Z^6 \bar{M}^2 - 4M_Z^4 \bar{M}^4 \right]^{\frac{1}{2}}}{2(\bar{M}^2 - M_Z^2)} .$$
(3.8)

Again, $C = 0$ in this case.

3. No $\gamma - Y$ mixing:

$$a_2 = b_2 = b_1 = \left[\frac{G\rho}{2\sqrt{2}} \cdot \frac{M_Z^2 M_Y^2}{M_Z^2 + M_Y^2} \right]^{\frac{1}{2}}$$

but

$$a_1 = b_1 \left[1 - \sin^2 \theta_W \cdot \frac{M_Y^2 + M_Z^2}{M_Y^2} \right] .$$
(3.9)

This last expression implies that

$$C = \frac{M_Z^2}{16M_Y^2}$$

which is consistent with the experimental limit of $C < 0.03$ if $M_Y > 1.5M_Z$.

The next two cases are the variances of cases 2 and 3 where we change the relative sign between b_1 and b_2 in Eq. (3.2) whereas other couplings are unchanged.

2'. $b_2 = -b_1$, otherwise same as in Eq. (3.8). In this case

$$C = \frac{(1 - 4 \sin^2 \theta_W)^2 M_Y^2 M_Z^2}{4(M_Y^2 + M_Z^2)^2} . \quad (3.10)$$

Since $\sin^2 \theta_W = 0.23$, the experimental constraint on $C < 0.03$ is automatically satisfied.

3'. $a_2 = -b_2 = b_1$, otherwise same as in Eq. (3.9). Now

$$C = \left(-2 + 4 \sin^2 \theta_W \frac{M_Y^2 + M_Z^2}{M_Y^2} \right)^2 \cdot \frac{M_Y^2 M_Z^2}{16(M_Y^2 + M_Z^2)^2} . \quad (3.11)$$

Again, the constraint on C is automatically satisfied.

Note that since in the last four cases we always have $|b_1| = |b_2|$. Equation (3.5) imposes on the Z mass the condition:

$$M_Z > \sqrt{2(\sqrt{2} - 1)} \bar{M} . \quad (3.12)$$

In the case of $\bar{M} = 100$ GeV, the extreme low value of M_Z is about 91 GeV.

4. Results and Discussions

In this section we study the finite-width and Y -boson effects on $e^+e^- \rightarrow \mu^+\mu^-$ total cross section and forward-backward asymmetry (see Appendix) in the energy range from 40 GeV to 60 GeV. We will first study the decoupled Y case. We will look at the effects due to Z width Γ_Z and the finite-width coefficient δ_Z . We then will study the combined Y and Z effects. In addition to Γ_Z and δ_Z , we now have to consider also the influence of the average mass \bar{M} and Z mass M_Z . These will be carried out for each of the four extreme cases that we mentioned at the end of the previous section.

4.1 DECOUPLED Y

In this case we only have one boson Z , and in the following illustrations we will take $M_Z = 92$ GeV. As can be seen from Fig. 2a the total cross section in this energy

range is insensitive to the Z width even up to $\Gamma_Z = 10$ GeV. Judging from this fact the total cross section is not an efficient tool in probing the difference between the gauge and non-gauge models. On the other hand, the effects are more substantiated in the forward-backward asymmetry, as can be seen from Fig. 2b. Thus from now on we will concentrate only on the asymmetries.

The naive way to look at the effect of Γ_Z on asymmetry is to assume the usual Breit-Wigner formula $M_Z^2 - s - iM_Z\Gamma_Z$. This is shown in Fig. 3a and Fig. 3b as solid curves. As explained in Sec. 2, this formula is not adequate in the case of broad resonances. Thus in the same figures we also give the results of the modified formula Eq. (2.14) with $\delta_Z = \Gamma_Z(M_Z^2)/\pi M_Z$, $\delta_Z = 0$ and $\delta_Z = -0.1$, respectively. Notice that the naive formula gives a much sharper dependence on the width effect. This is because at $\sqrt{s} = 45$ GeV (Fig. 3a) and $\sqrt{s} = 60$ GeV (Fig. 3b) $\Gamma_Z(s)$ are smaller than $\Gamma_Z(M_Z^2)$ due to phase space effects. Furthermore, the asymmetry effects due to the closed channels through δ_Z can be at most ± 0.01 at $\sqrt{s} = 45$ GeV and ± 0.03 at $\sqrt{s} = 60$ GeV. One may worry about the effect due to different values of $\sin^2\theta_W$. Our calculations for $\sin^2\theta_W = 0.23 \pm 0.02$ show that the asymmetry can change by no more than ± 0.001 at $\sqrt{s} = 45$ GeV and ± 0.005 at $\sqrt{s} = 60$ GeV.

4.2 COMBINED Y AND Z EFFECTS

Now we fix the average mass at $\bar{M} = 100$ GeV and $M_Z = 92$ GeV to study the combined Y and Z effects with both δ 's chosen to be $\delta = \Gamma(M^2)/\pi M$. The asymmetries for cases 2, 2', 3, 3' are calculated in comparison with case 1, and the results for $\sqrt{s} = 45$ GeV and $\sqrt{s} = 60$ GeV are shown in Fig. 4a and Fig. 4b, respectively. Notice that the curves of combined Y and Z cases lie consistently above the single Z case at $\sqrt{s} = 45$ GeV. This is because for all cases, $M_Z = 92$ GeV thus for combined Y and Z the \bar{M} is higher. At $\sqrt{s} = 60$ GeV as we are closer to the resonance peak the width effects (especially for large Γ) become stronger and the

asymmetry effects are larger, but the essential features are the same. We find that the difference in asymmetries between the extreme combinations in cases 2, 2', 3, 3' and the single Z case runs from 0.003 to 0.007 at $\sqrt{s} = 45$ GeV and from 0.010 to 0.025 at $\sqrt{s} = 60$ GeV.

Next we look at the effect of the average mass \bar{M} . This is shown in Fig. 5a and 5b for the case 2 as compared to the single Z case ($M_Z = 92$ GeV) by varying \bar{M} from 92 GeV to 100 GeV and taking M_Z close to the minimal value given by Eq. (3.12). Varying \bar{M} around the standard Z mass, for example from 92 GeV to 96 GeV, leads to a change of the asymmetry by +0.004 at $\sqrt{s} = 45$ GeV and +0.012 at $\sqrt{s} = 60$ GeV.

4.3 CONCLUSION

To summarize our calculations we plot the asymmetry versus the width Γ_Z at $\sqrt{s} = 45$ GeV (Fig. 6a) and $\sqrt{s} = 60$ GeV (Fig. 6b) for the extreme cases, namely for the decoupled Y case (single Z) and for “no $\gamma - Y$ mixing” cases with opposite signs in the axial-vector couplings (i.e., cases 3 and 3'). In each case we present it as a band allowing for the extreme values of the finite width coefficient δ (i.e., to vary δ between -0.1 and $\Gamma/\pi M$). The dots on the Y -axis in Fig. 6a and 6b represent the predictions from the standard model with a width $\Gamma = 3$ GeV.

It can be seen from these two figures that the composite models accommodate an asymmetry value between -0.165 and -0.180 at $\sqrt{s} = 45$ GeV, and between -0.348 and -0.396 at $\sqrt{s} = 60$ GeV. This large range of asymmetry values are chiefly due to the combined effects of the existence of Y -boson and the possible large widths of Y and Z bosons. If the experimental value deviates from -0.178 at $\sqrt{s} = 45$ GeV but still lies within the range $(-0.165, -0.178)$, and if one insists on narrow width of the neutral boson, then the composite model can accommodate it by having a Y boson or strong closed channels for the Z . But if the asymmetry lies outside this range while

still within $(-0.164, -0.180)$ then a broader width should be invoked.

The situation is similar when $\sqrt{s} = 60$ GeV (Fig. 6b). However, the asymmetry effect is much more pronounced allowing for the distinction among the models without requiring the same level of experimental accuracy.

Although the original purpose of our calculation was to estimate the observability of large width effects of neutral bosons, it turns out that due to the large variety of free parameters inherent in all models this issue is not very unique. As mentioned above the large effects following from naive treatment of width (Breit-Wigner formula) are largely cancelled by phase space effects which in turn might be counterbalanced by the existence of the closed channels and a possible Y boson. Our results indicate the advisability of certain caution when dealing with these sorts of effects.

A realistic analysis of our Fig. 6 a) and b) shows that the chances for experimental elimination of most models in the near future are rather slim. However, we believe that our curves may serve as good reference for future experiments since any precise measurement of asymmetry should eliminate a major domain in parameter space. It is conceivable that an independent information then might lead to an ultimate elimination of this ambiguity.

In this paper we have limited our attention to the unpolarized asymmetry associated with leptons. As is well known, much larger effects should be expected in $e^+e^- \rightarrow q\bar{q}$ processes. The price one has to pay there is the necessity of a unique parent quark identification which reduces statistics enormously. Furthermore, the polarization effects can give some independent constraints on the neutral current structure. These seem to be the useful areas of future development of this program.

Acknowledgements

The authors thank Professor S. D. Drell for his hospitality in the SLAC Theory Group.

Appendix

For the sake of completeness we list in this appendix the formulae for differential and integrated cross sections and for the forward-backward asymmetry. We shall neglect electron mass everywhere but the mass of final state, m_f , will be kept through the velocity $\beta_f = \sqrt{1 - 4m_f^2/s}$.

Using the approximations (2.18) and (2.19) and denoting photon term by subscript 0 we get the differential cross section for a general reaction $e^+e^- \rightarrow f\bar{f}$ proceeding through the exchange of a photon and n neutral weak bosons

$$\frac{d\sigma}{d\cos\theta} = \sum_{i=0}^n \sum_{j=i}^n c_{ij} d_{ij} (f_{ij} + g_{ij} \cos\theta + h_{ij} \cos^2\theta) \quad (i, j = 0, 1, \dots, n) \quad (\text{A.1})$$

where

$$c_{00} = \frac{\pi\alpha^2 Q_f^2 \beta_f}{2s} \quad , \quad (\text{A.2})$$

$$c_{0j} = -\frac{\alpha Q_f \beta_f}{4} \quad (j \neq 0) \quad , \quad (\text{A.3})$$

$$c_{ii} = \frac{s\beta_f}{32\pi} \quad , \quad (\text{A.4})$$

$$c_{ij} = \frac{s\beta_f}{16\pi} \quad (i \neq j ; i, j \neq 0) \quad , \quad (\text{A.5})$$

$$d_{00} = 1 \quad , \quad (\text{A.6})$$

$$d_{0j} = \frac{(1 + \delta_i)(s - M_i^2 - \Pi_i(s))}{(s - M_i^2 - \Pi_i(s))^2 + (\Gamma_i(s)M_i)^2} \quad (j \neq 0) \quad , \quad (\text{A.7})$$

$$d_{ii} = \frac{1 + \delta_i}{(s - M_i^2 - \Pi_i(s))^2 + (\Gamma_i(s)M_i)^2} \quad (i \neq 0) \quad , \quad (\text{A.8})$$

$$d_{ij} = \frac{(1 + \delta_i)(1 + \delta_j)[(s - M_i^2 - \Pi_i(s))[(s - M_j^2 - \Pi_j(s))]]}{[(s - M_i^2 - \Pi_i(s))^2 + (\Gamma_i(s)M_i)^2][(s - M_j^2 - \Pi_j(s))^2 + (\Gamma_j(s)M_j)^2]} \quad (j \neq i ; i, j \neq 0) \quad , \quad (\text{A.9})$$

$$f_{00} = 2 - \beta_f^2 , \quad (\text{A.10})$$

$$f_{0j} = a_{ej}a_{fj}(2 - \beta_f^2) \quad (j \neq 0) , \quad (\text{A.11})$$

$$f_{ii} = (2 - \beta_f^2)(a_{ei}^2 a_{fi}^2 + b_{ei}^2 a_{fi}^2) + \beta_f^2(a_{ei}^2 b_{fi}^2 + b_{ei}^2 b_{fi}^2) \quad (i \neq 0) , \quad (\text{A.12})$$

$$f_{ij} = (a_{ei}a_{ej} + b_{ei}b_{ej}) \left[(2 - \beta_f^2)a_{fi}a_{fj} + \beta_f^2 b_{fi}b_{fj} \right] \quad (i \neq j ; i, j \neq 0) , \quad (\text{A.13})$$

$$g_{00} = 0 , \quad (\text{A.14})$$

$$g_{0j} = 2\beta_f b_{ei}b_{fi} \quad (j \neq 0) , \quad (\text{A.15})$$

$$g_{ii} = 8\beta_f a_{ei}b_{ei}a_{fi}b_{fi} \quad (i \neq 0) , \quad (\text{A.16})$$

$$g_{ij} = 2\beta_f (a_{ej}b_{ei} + a_{ei}b_{ej})(a_{fj}b_{fi} + a_{fi}b_{fj}) \quad (i \neq j ; i, j \neq 0) , \quad (\text{A.17})$$

$$h_{00} = \beta_f^2 , \quad (\text{A.18})$$

$$h_{0j} = \beta_f^2 a_{ei}a_{fi} \quad (j \neq 0) , \quad (\text{A.19})$$

$$h_{ii} = \beta_f^2 (a_{ei}^2 + b_{ei}^2)(a_{fi}^2 + b_{fi}^2) \quad (i \neq 0) , \quad (\text{A.20})$$

$$h_{ij} = \beta_f^2 (a_{ei}a_{ej} + b_{ei}b_{ej})(a_{fi}a_{fj} + b_{fi}b_{fj}) \quad (j \neq i ; i, j \neq 0) . \quad (\text{A.21})$$

All symbols in the formulae above are as defined in (2.15), the indices e and f at the couplings indicate couplings to electrons or final state particle f .

In the general case when the small forward and backward cones with opening angles $2\theta_0$ are not covered by detector we get for the total integrated cross section

$$\sigma^{tot}(\theta_0) = 2 \sum_{i=0}^n \sum_{j=i}^n c_{ij} d_{ij} \left[f_{ij} \cos\theta_0 + \frac{1}{3} h_{ij} \cos^3\theta_0 \right] \quad (\text{A.22})$$

and for the global forward-backward asymmetry




$$A_{FB}(\theta_0) = \frac{1}{\sigma^{tot}(\theta_0)} \sum_{i=0}^n \sum_{j=1}^n c_{ij} d_{ij} g_{ij} \cos^2\theta_0 . \quad (\text{A.23})$$

All examples in our paper are calculated for $\theta_0 = 0$.

References

1. UA1 Coll., G. Arnison *et al.*, Phys. Lett. 122B (1983) 189; *ibid.*, 126B (1983) 189.
UA2 Coll., M. Banner *et al.*, *ibid.* 122B (1983) 476.
P. Bagnala *et al.*, *ibid.* 129B (1983) 130.
2. For review see H. Harari, Lect. given at SLAC Summer Institute 1982.
Also appear in "Electroweak Interactions at High Energies," Proc. of the 1982 DESY Workshop, ed. R. Kögerler and D. Schildknecht, World Scientific (Singapore), p. 334.
3. L. Abbott and E. Farhi, Phys. Lett. 101B (1981) 69.
4. H. Fritzsch and G. Mandelbaum, Phys. Lett. 102B (1981) 319.
5. W. Hollik, Z. Phys. C8 (1981) 149. Earlier references can be found therein.
6. G. J. Gounaris and J. J. Sakurai, Phys. Rev. Lett. 21 (1968) 244.
F. M. Renard, Nucl. Phys. B15 (1970) 118; Phys. Lett. 47B (1973) 361; Nucl. Phys. B82 (1979) 1.
7. M. Veltman, Nucl. Phys. B123 (1977) 89.
M. Capdequi-Peyranère, F. M. Renard and M. Talon, Z. Phys. C5 (1980) 337.
8. E. M. deGroot and D. Schildknecht, Z. Phys. C10 (1981) 55.
9. P. Chen and F. M. Renard, SLAC-PUB-3049 (1983).
10. J. D. Bjorken, Phys. Rev. D 19 (1979) 335.
P. Q. Hung and J. J. Sakurai, Nucl. Phys. B143 (1978) 81.
M. Kuroda and D. Schildknecht, Phys. Lett. 121B (1983) 173.
R. Kögerler and D. Schildknecht, CERN-TH3231 (1982).

Figure Captions

1. Diagrams contributing to $\Sigma(s)$.
2. a) $\sigma(e^+e^- \rightarrow \mu^+\mu^-)$ and b) asymmetry in the single Z boson case ($M_Z = 92$ GeV) versus total center-of-mass energy. Solid line: $\Gamma_Z = 3$ GeV, $\delta_Z = \Gamma_Z/\pi M_Z$; dotted line: $\Gamma_Z = 10$ GeV, $\delta_Z = \Gamma_Z/\pi M_Z$; dashed line: $\Gamma_Z = 10$ GeV, Breit-Wigner case. The sections of the σ and the asymmetry ranging from 55 GeV to 60 GeV are magnified and shown in the insertions, respectively.
3. Asymmetry in the single Z boson case ($M_Z = 92$ GeV) versus Γ_Z at a) $\sqrt{s} = 45$ GeV and b) $\sqrt{s} = 60$ GeV. Solid curve corresponds to Breit-Wigner, dotted to $\delta_Z = \Gamma_Z/\pi M_Z$, dashed to $\delta_Z = 0$ and dash-dotted to $\delta_Z = -0.1$.
4. Asymmetry versus Γ_Z in the combined Z, Y cases at a) $\sqrt{s} = 45$ GeV and b) $\sqrt{s} = 60$ GeV. The five cases are described in Sec. 3.
5. Asymmetry versus \bar{M} in the combined Z, Y cases at a) $\sqrt{s} = 45$ GeV and b) $\sqrt{s} = 60$ GeV. Solid and dotted curves correspond to case 1 with $\Gamma_Z = 3$ and 10 GeV, respectively, and dashed and dash-dotted curves correspond to case 2.
6. Asymmetry versus Γ_Z in the combined Z, Y cases at a) $\sqrt{s} = 45$ GeV and b) $\sqrt{s} = 60$ GeV; shaded areas are obtained by varying δ between -0.1 and $\frac{\Gamma}{\pi M}$.
 - Standard model ($\Gamma_Z = 3$ GeV)
 -  Case 1 (see Sec. 3)
 -  Case 3
 -  Case 3'

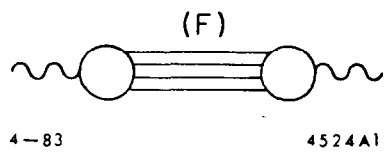


Fig. 1

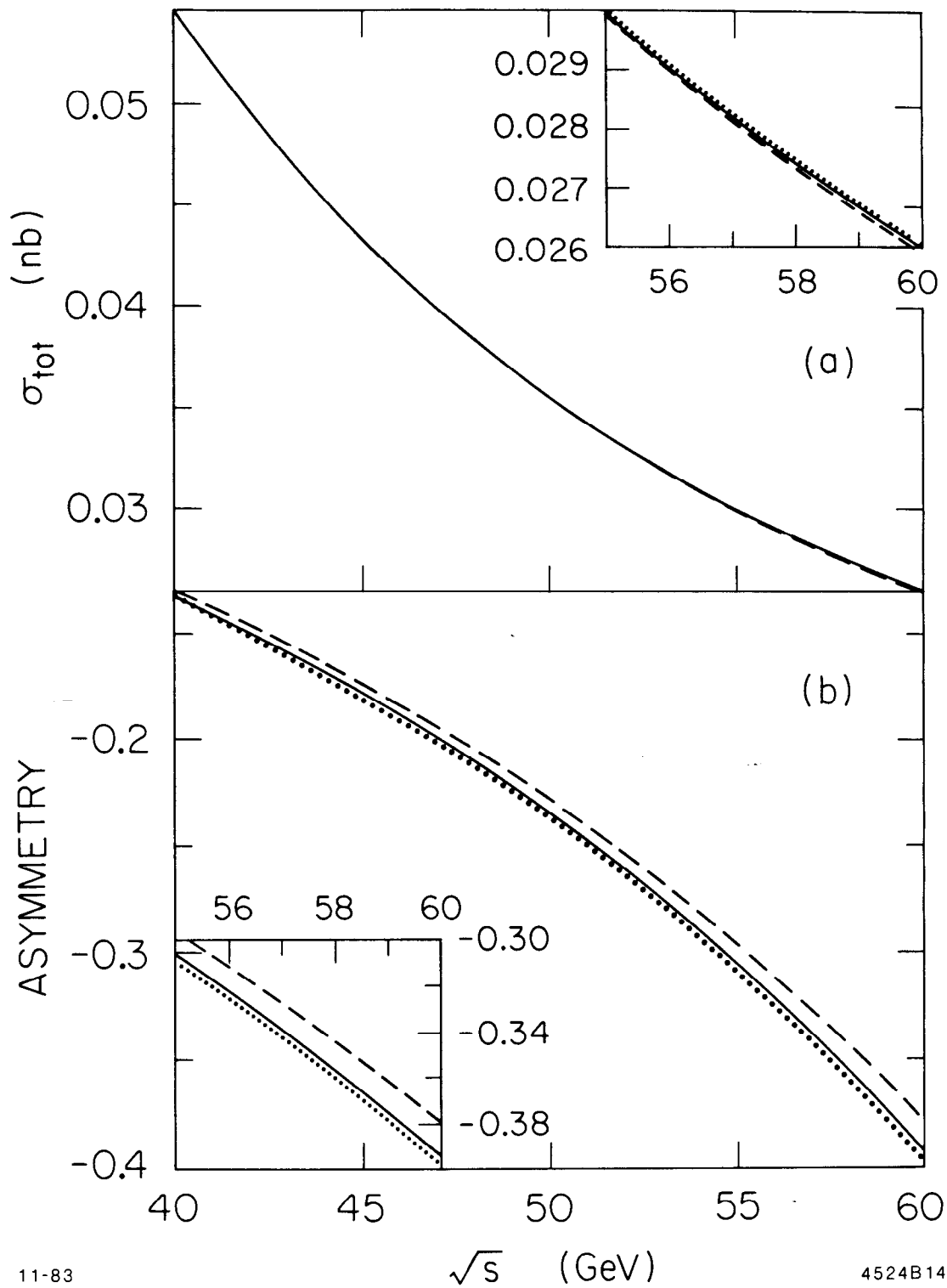


Fig. 2

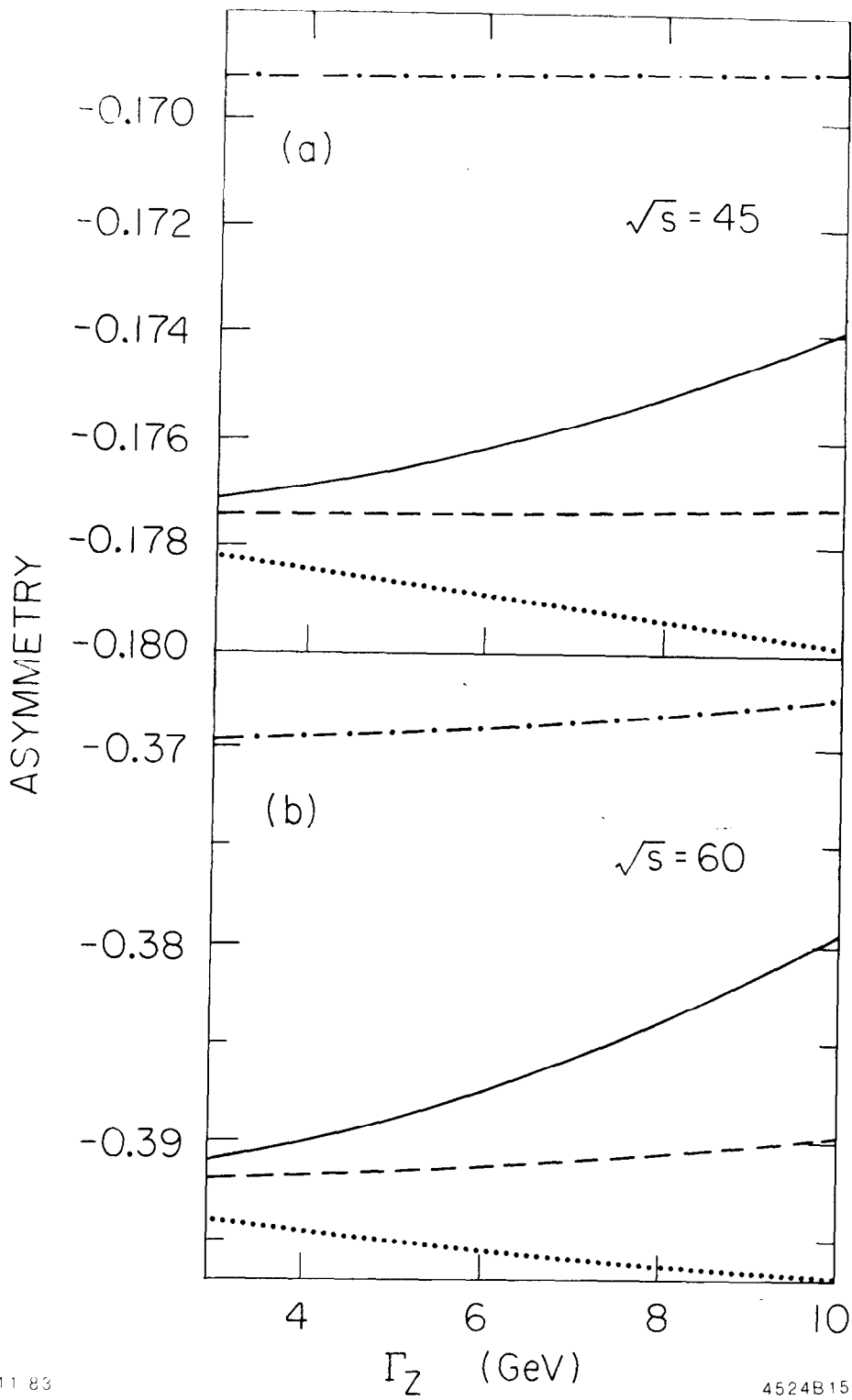
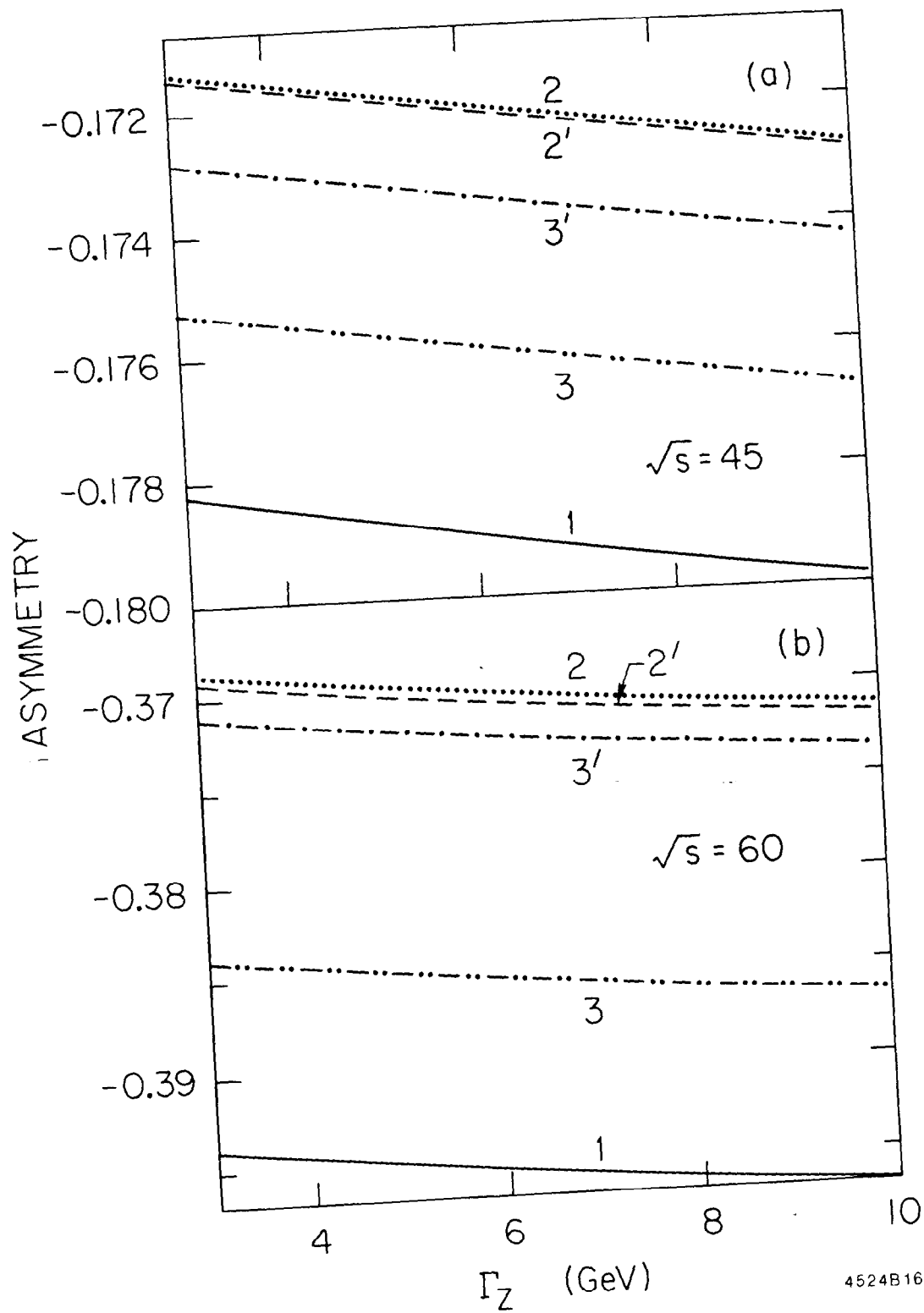


Fig. 3



11-83

4524B16

Fig. 4

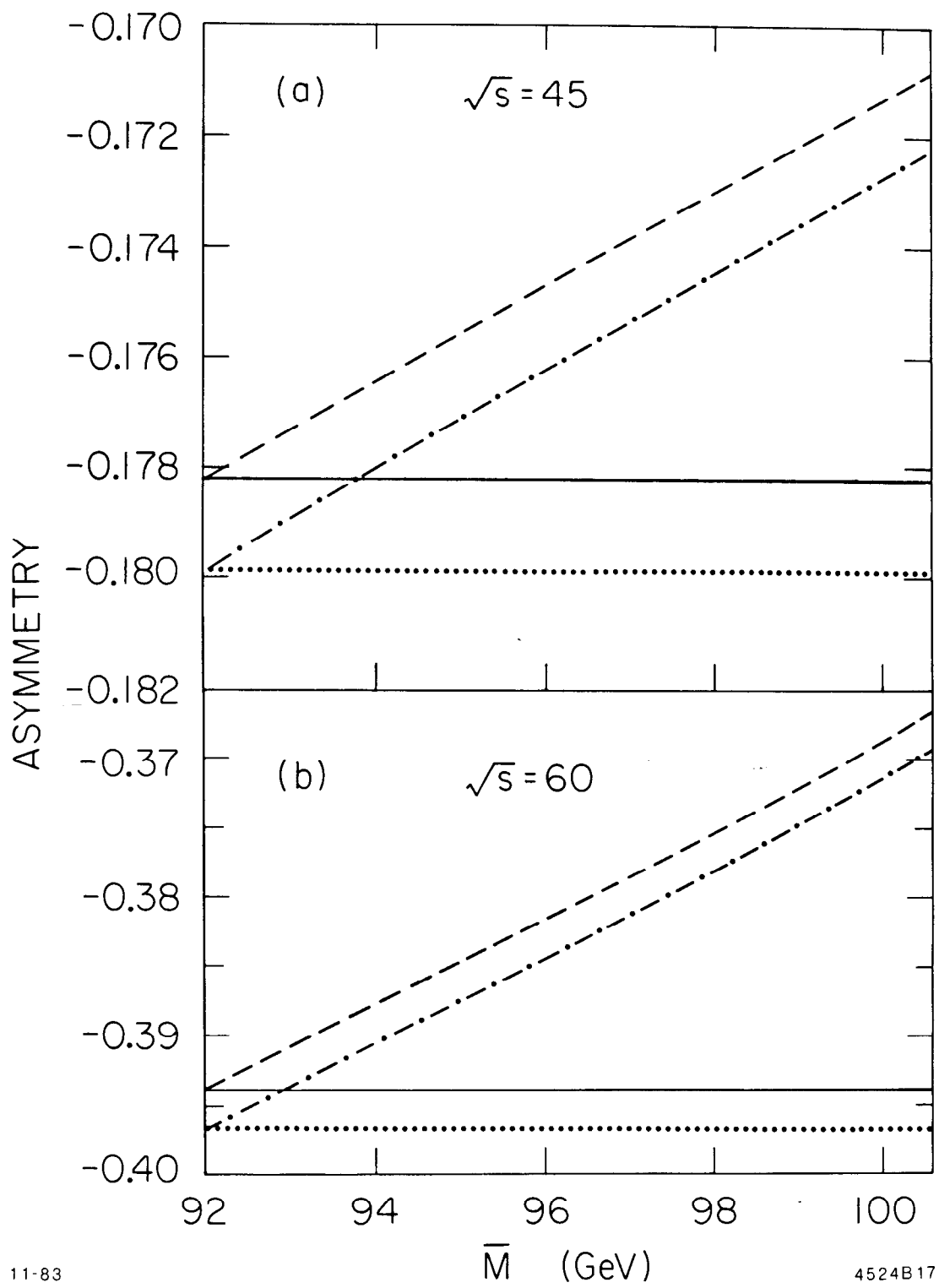
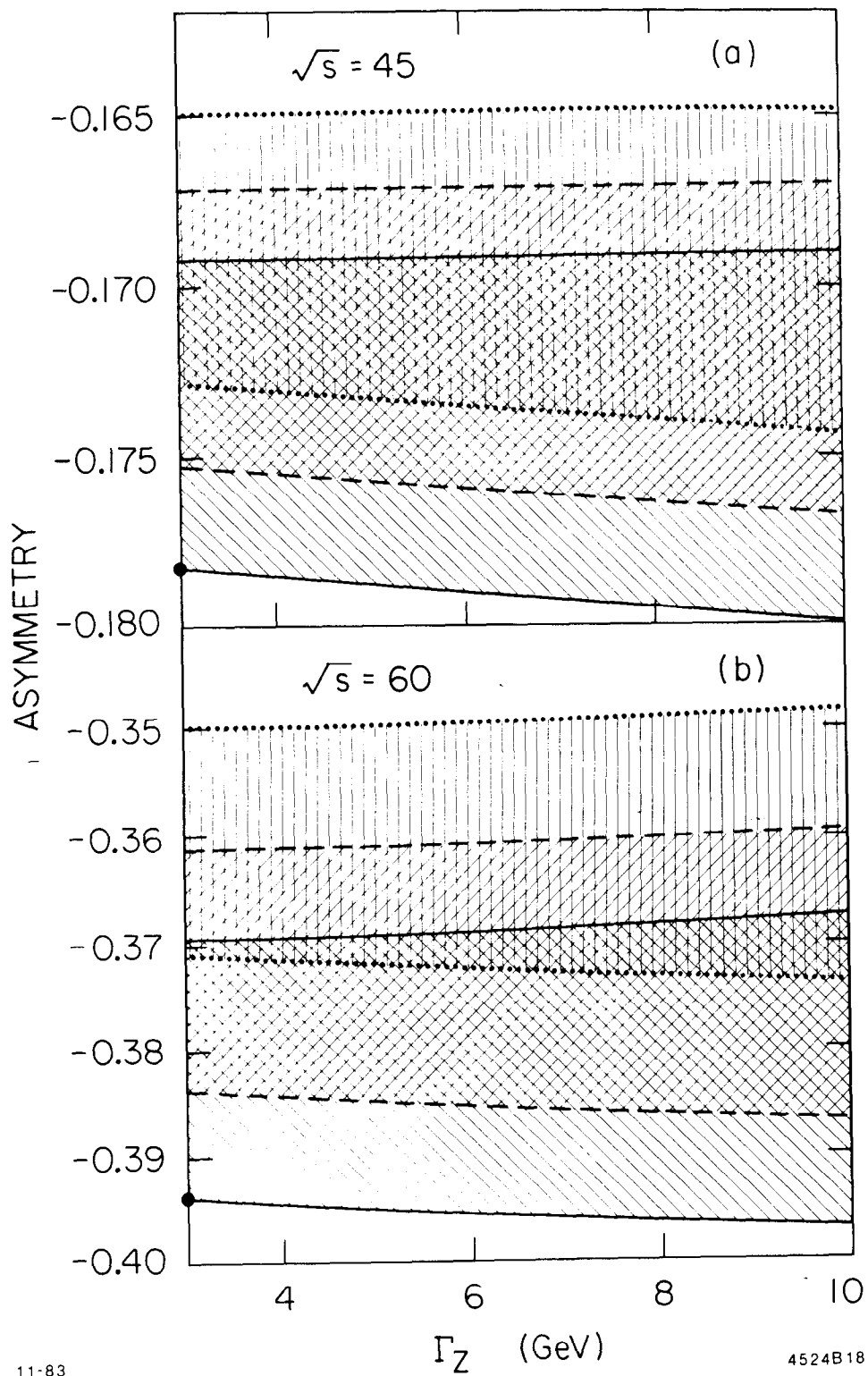


Fig. 5



11-83

4524B18

Fig. 6